

Wang, X., et al., 2023, Molybdenum isotope signature of microbial nitrogen utilization in siboglinid tubeworms: *Geology*, <https://doi.org/10.1130/G51077.1>

## Supplemental Material

**Materials and Methods**

**Tables S1–S5**

**Figure S1**

**References**

# Molybdenum isotope signature of microbial nitrogen utilization in siboglinid tubeworms

Xudong Wang, Ting Xu, Jörn Peckmann, Germain Bayon, Zice Jia, Shanggui Gong, Jie Li, Erik Cordes, Yanan Sun, Jun Tao, Duofu Chen, Dong Feng

## MATERIALS AND METHODS

### Geological setting and sample collection

The Haima seeps are located in the Qiongdongnan basin on the northwestern part of the South China Sea (Fig. 1A). So far, various individual seep sites have been discovered in this area of about 350 km<sup>2</sup>. Tubeworms assigned to *Paraescarpia echinospica* (Guan et al., 2021) were collected by ROV *Haima* at approximately 1390 m water depth from the Haima seeps during cruises in September 2020 (Table S1; Fig. 1B and 1C).

### Segmentation of the chitinous tube of *Paraescarpia echinospica*

An approximately 44.5 cm long chitinous tube of the seep-dwelling tubeworm *Paraescarpia echinospica* was divided into 19 sub-samples with a ceramic knife to avoid metal pollution (see Table S2 for details). From anterior to posterior end, the soft tissue of tubeworms is subdivided into plume, vestimentum, trophosome, and opisthosome (Minic and Hervé, 2004). Based on a previous study of the same type of samples from the same area and the physiological traits of *P. echinospica* (Southward et al., 2002; Guan et al., 2021), we allocated obturaculum and vestimentum to sections P1-P3, trophosome to sections P4-P19 section of the chitinous tube (including the tail end vacancy, see Fig. 1D). The spatial correspondence between soft tissue and chitinous tube is not accurate since the worm moves inside the tube. The anterior end (P1-P16) of the tubeworm immerses into seawater to obtain oxygen with the plume, while the posterior end (P17-P19), rooted in the sediment, takes up hydrogen sulfide. Through the circulation system of the host involving hemoglobin, the obtained oxygen and hydrogen sulfide are transported to the trophosome, where symbiotic bacteria produce carbon and nutrition sources provided to the host (Sun et al., 2021).

### Trace element analyses

The samples were put into an acid-washed 50 ml centrifuge tube with 20 ml ultrapure water (and a small amount of acetic acid) and were shaken for four times (each for half an hour) to remove any terrigenous detritus adsorbed to the surface of the tube. After the cleaning procedure, the studied chitinous tube was observed under a stereoscope to ensure that the surface of the chitinous tube is clean and free of adsorbents.

The samples were then transferred into an acid-washed 30 ml Teflon beaker and soaked in 2 ml aqua regia (0.5 ml conc. HNO<sub>3</sub> + 1.5 ml conc. HCl). The lid of the Teflon beaker was open to avoid gas generation and accumulation. After overnight reaction, 2 ml aqua regia were added to ensure that the samples were completely dissolved. After digestion and evaporation, the samples were dissolved in 10 M H<sub>2</sub>O<sub>2</sub> (drop by drop until no more bubbles evolved) and evaporated overnight. The samples were finally re-dissolved in 4 ml 2 N HNO<sub>3</sub> (constant volume, mother solution), and a small amount of solution (diluted mother solution) with added internal standard was used for analyzing trace elements with ICP-MS.

Internal standard: 60 ppb Rh, In, Re, Bi

Instrument: ICP-MS, Thermo Fisher X Series 2

Standard samples: BHVO-2, W-2a and molybdenum single standard solution

Analytical error: ≤ 5%.

Trace element contents of the chitinous tube are reported on dry matter basis, all trace elements were analyzed by Guizhou Tongwei Analytical Technology Co., Ltd.

### **Molybdenum (Mo) isotope analyses**

The sample treatment for Mo isotope analysis was processed by Guizhou Tongwei Analytical Technology Co., Ltd. Before analyzing the Mo isotope composition of samples, it was necessary to separate and purify Mo to eliminate the influence of interfering elements on Mo isotopes (such as the allotropic isotopes <sup>92</sup>Zr, <sup>94</sup>Zr, <sup>96</sup>Zr, <sup>96</sup>Ru, <sup>98</sup>Ru, and <sup>100</sup>Ru, and Fe or Mn interfering with the carrier gas Ar). All samples were dissolved in 3 ml 1 N HCl (a constant volume) before loading onto the column.

For Mo isotope purification methods, readers are referred to Li et al. (2014). According to the Mo concentration of the sample, the weight of the sample was determined. Generally, 90 ng of pure Mo is sufficient to meet the analytical requirement. The same amount (i.e. 90 ng) of <sup>97</sup>Mo-<sup>100</sup>Mo double spike was added, and a special BPHA chelating resin was used to separate and purify Mo. After complete separation of Mo in the sample, the solution was collected into a clean Teflon beaker. After digestion with the lid open and evaporation on a 120°C hot plate, the solid residue was repeatedly dissolved with concentrated HNO<sub>3</sub> and H<sub>2</sub>O<sub>2</sub> until the organic matter was completely digested. After that, a drop of concentrated HNO<sub>3</sub> and 0.5 ml ultrapure water was added into the Teflon beaker. The samples were filtered (0.45 μm membrane) to avoid any potential solid residue and diluted to 1 ml (constant volume) for analysis. The determination of the Mo isotope ratio was achieved in the State Key Laboratory of Isotope Geochemistry, Guangzhou Institute of Geochemistry, Chinese Academy of Sciences. The analysis was conducted using a Thermo Fisher Scientific Neptune Multi-Collector Inductively Coupled Plasma Mass Spectrometer (MC-ICP-MS). All procedures were completed in an ultra-clean room. The blank of the process was 0.07 to 0.23 ng (n=4), which is less than 1% of total Mo processed in the chemical treatment.

Before analyzing the samples, the standard solution (NIST SRM 3134) was analyzed five times to check the background signal of the MC-ICP-MS. NIST SRM 3134 is the approved Mo isotope standard, and the difference between NIST SRM 3134 and the former Mo standard solution (Johnson–Matthey Spec Pure, JMC) is 0.25‰

(Siebert et al., 2003). Therefore, the data of this study will be uniformly equal to NIST SRM 3134 = 0.25‰. The calculation formula of Mo isotope is as follow:

$$\delta^{98/95}\text{Mo} (\text{‰}) = \left( \frac{{}^{98/95}\text{Mo}_{\text{sample}}}{{}^{98/95}\text{Mo}_{\text{NIST3134}} * 0.99975} - 1 \right) * 1000$$

A standard sample (NIST SRM 3134) was inserted during analyses of every five samples for instrument stability evaluation. Isotope calculation was completed by MATLAB program designed by Zhang et al. (2015).

## SUPPLEMENTARY TABLES

Table S1. Sample information.

Site	Haima seep, northwestern South China Sea
Latitude	16.73°N
Longitude	110.48°E
Water depth (m)	1390
Sampling date	2020.09
Species	<i>Paraescarpia echinospica</i>
Chemotrophic symbionts	Thiotrophs
Total tube length	44.5 cm

Table S2. Section of tubeworm *Paraescarpia echinospica* used in this study.

Sub sample ID	Corresponding tube length (cm)
P1	0-1.5
P2	1.5-3.0
P3	3.0-4.5
P4	4.5-6.0
P5	6.0-8.5
P6	8.5-11.0
P7	11.0-13.5
P8	13.5-16.0
P9	16.0-18.5
P10	18.5-21.0
P11	21.0-23.5
P12	23.5-26.0
P13	26.0-28.5
P14	28.5-31.0
P15	31.0-33.5
P16	33.5-36.0
P17	36.0-38.5
P18	38.5-41.0
P19	41.0-44.5

Table S3. Trace element contents (in  $\mu\text{g/g}$ ) for the tube sections.

Sub sample ID	V	Mn	Fe	Co	Ni	Cu	Zn	Sr	Mo	U
P1	9.66	105	445	0.47	152	61.0	123	31.2	0.66	0.58
P2	22.0	166	200	0.31	194	48.5	108	24.7	0.96	0.97
P3	26.3	25.2	310	0.28	109	21.4	63.0	23.5	1.45	1.51
P4	26.6	14.6	222	0.19	78.1	15.6	49.0	16.2	0.95	1.80
P5	26.9	3.68	108	0.09	41.0	7.44	24.4	14.8	0.86	2.43
P6	22.6	4.80	90.7	0.11	44.5	8.48	35.4	12.2	0.94	2.52
P7	18.3	4.21	67.8	0.12	39.3	7.02	37.9	9.45	0.91	2.40
P8	13.8	2.70	63.8	0.12	31.5	5.39	34.3	6.78	0.69	2.16
P9	8.72	2.63	123	0.40	38.3	6.29	44.1	4.68	0.49	1.33
P10	7.32	8.75	193	0.99	43.7	10.0	51.7	5.26	0.46	1.00
P11	7.99	0.86	55.1	0.23	29.2	3.99	33.8	1.97	0.43	0.82
P12	10.3	1.13	42.8	0.11	24.3	3.62	32.2	1.53	0.45	0.78
P13	10.8	1.30	53.6	0.09	18.7	3.11	32.0	1.21	0.34	0.69
P14	15.5	1.05	18.3	0.04	19.3	2.35	33.1	0.54	0.34	0.75
P15	21.5	1.63	41.1	0.12	34.0	3.66	45.5	0.68	0.40	1.05
P16	20.1	0.78	75.1	0.80	64.7	7.26	49.8	0.24	1.60	3.10
P17	42.3	31.0	164	1.66	95.5	25.7	131	1.02	9.84	2.45
P18	49.9	37.5	304	1.77	139	32.3	198	1.26	17.7	1.32
P19	49.4	6.10	299	1.89	159	50.0	231	0.61	24.2	1.86

Table S3 (continued)

Sub sample ID	La	Ce	Pr	Nd	Sm	Eu	Gd	Tb	Dy	Y	Ho	Er	Tm	Yb	Lu
P1	382	674	82.9	329	70.6	15.2	68.8	10.1	56.7	407	11.9	33.8	5.35	36.2	6.55
P2	106	187	25.0	107	24.6	5.78	29.3	4.42	27.6	242	6.50	20.4	3.52	25.0	4.47
P3	72.1	111	17.8	81.1	19.8	4.98	25.2	3.88	24.2	432	6.05	19.4	3.25	22.7	4.16
P4	73.5	138	17.5	75.7	18.7	4.30	19.7	3.00	18.9	511	4.43	14.2	2.37	15.8	2.90
P5	41.0	64.5	10.5	46.7	11.3	2.77	13.7	2.09	14.4	201	3.45	11.1	1.89	13.1	2.40
P6	39.6	65.4	9.80	44.0	10.1	2.49	12.2	1.87	11.9	137	3.00	9.40	1.54	11.5	2.21
P7	41.7	69.0	10.2	42.9	10.1	2.45	12.0	1.80	11.9	280	2.86	10.5	1.57	10.8	2.04
P8	19.9	28.7	4.87	22.4	5.91	1.45	7.10	1.20	8.04	61.3	2.02	6.99	1.08	8.33	1.56
P9	30.8	54.1	7.85	32.2	7.31	1.72	8.39	1.33	8.20	52.2	1.86	5.66	0.96	6.59	1.24
P10	51.3	88.9	12.3	53.4	11.6	2.84	13.8	2.04	12.2	82.9	3.00	7.94	1.33	8.91	1.54
P11	12.2	17.1	2.89	12.5	2.91	0.86	3.98	0.56	3.67	24.6	0.94	3.28	0.52	3.68	0.71
P12	17.0	26.9	3.75	15.7	3.94	0.85	3.80	0.66	3.92	25.2	0.86	2.75	0.47	3.52	0.69
P13	34.2	57.9	7.83	29.6	5.72	1.33	5.52	0.84	4.96	28.9	1.04	3.24	0.53	3.63	0.68
P14	10.2	13.3	1.85	6.88	1.60	0.42	2.15	0.37	1.89	12.3	0.43	1.82	0.28	1.97	0.43
P15	14.1	22.2	3.03	11.7	2.67	0.63	3.18	0.50	3.12	20.2	0.72	2.16	0.38	2.98	0.45
P16	19.2	31.1	5.13	18.7	4.99	1.18	4.38	0.91	6.07	37.8	1.21	4.21	0.93	6.46	1.07
P17	87.7	236	18.4	79.2	19.3	3.79	22.4	3.62	22.0	121	4.17	13.2	2.11	14.7	2.73
P18	111	164	20.7	78.9	19.2	4.48	19.0	2.84	18.0	114	4.16	12.4	1.88	12.0	2.00
P19	83.0	128	15.2	69.3	15.4	4.25	17.9	2.71	16.5	103	3.12	9.27	1.64	13.7	2.32

Table S4. Mo isotopes for the tube sections, porewater and sediment.

Sample ID	$\delta^{98}\text{Mo}$ (‰, NIST = 0.25 ‰)	2SE
P1	0.44	0.03
P2	-1.10	0.04
P3	-1.36	0.04
P4	-4.59	0.05
P5	-4.22	0.05
P6	-2.64	0.05
P7	-1.69	0.03
P8	-1.10	0.04
P9	-3.00	0.07
P10	-1.96	0.06
P11	-1.41	0.06
P12	-0.82	0.05
P13	-1.89	0.04
P14	-0.20	0.04
P15	-0.78	0.06
P16	0.71	0.04
P17	1.29	0.03
P18	1.50	0.09
P19	1.40	0.03
porewater QDN-PC01	1.75	0.09
porewater QDN-PC02	0.98	0.11
sediment ROV02-PC01	1.17	0.03

Table S5. Summary of Mo isotopes from various natural material.

No.	Reservoir	Sample	$\delta^{98}\text{Mo}$ (min)	$\delta^{98}\text{Mo}$ (max)	Reference
1	Geological body	Chondrites	0	0.4	Kendall et al., 2017
2		Iron meteorites	0.1	0.5	
3		Achondrites	-0.8	0.5	
4		Komatiites	-0.2	0.3	
5		Crustal igneous rocks (felsic to mafic)	-0.2	0.6	
6		Molybdenites	-1.4	2.4	
7	Marine system	Euxinic organic-rich mudrocks	-1.3	2.4	Chen et al., 2022
8		Marine sediments	-1.71	2.3	
9		Seawater	2.1	2.3	
10		iron-manganese oxides	-1.5	-0.4	
11		Recent euxinic sediments	1.0	2.3	
12		Suboxic pore fluids	1.7	3.6	
13		Precambrian carbonates (stromatolites)	-1.54	1.22	
14		Early Mesoproterozoic marine carbonate	-4.00	2.51	
15	(Micro-)organisms	Bivalves	1.18	2.31	Anbar, 2004
16		Gastropods	0.92	2.12	
17		Serpulid tube	0.9		
18		Corals	0.46	2.19	
19		Cyanobacterial nitrate utilization and N <sub>2</sub> fixation	1.05	2.10	
20		Seep tubeworm ( <i>Paraescarpia echinospica</i> )	-4.59	1.50	
					Thoby et al., 2021
					Luo et al., 2021
					Voegelin et al., 2009
					Wang et al., 2019
					Zerkle et al., 2011
					This study

**SUPPLEMENTARY FIGURE**

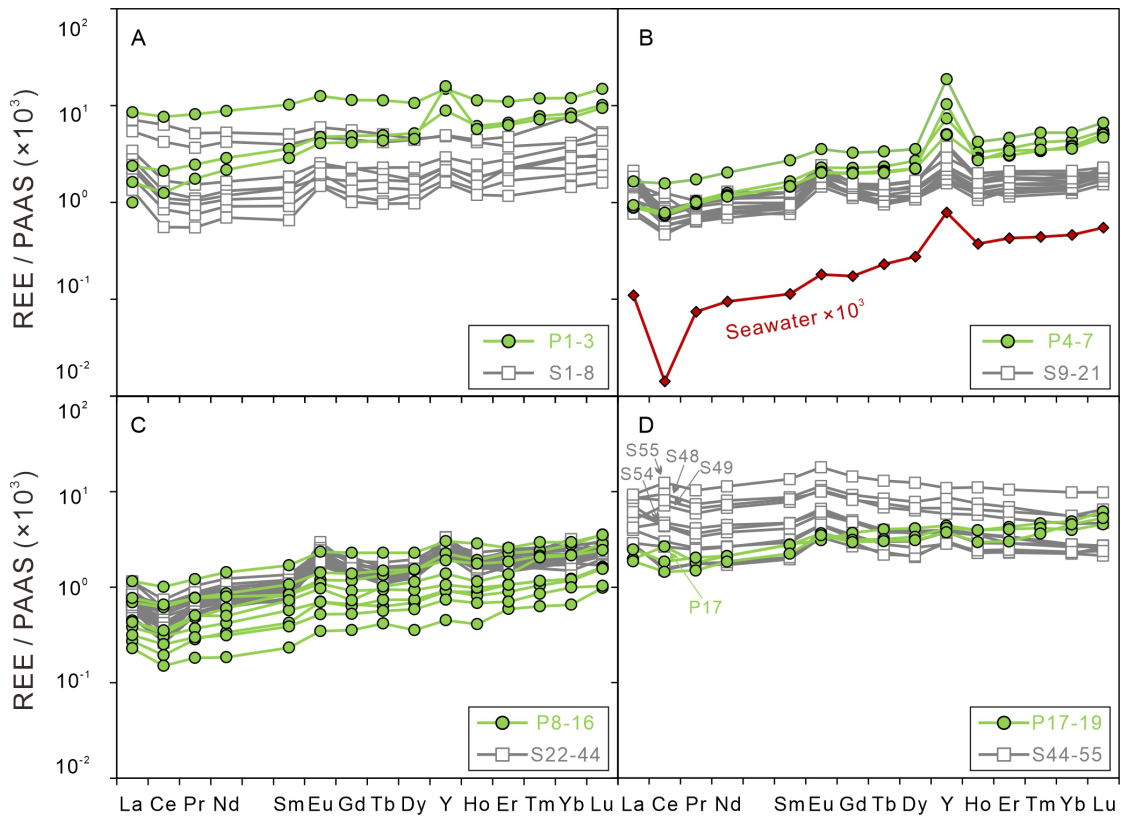


Figure S1. Shale-normalized (PAAS; Pourmand et al., 2012) rare earth element patterns: (A) sections P1-3, (B) sections P4-7 and seawater from the South China Sea (red diamond, water depth: 1488 m; Alibo and Nozaki, 2000), (C) sections P8-16 and (D) sections P17-19 of the chitinous tube of *Paraescarpia echinospica* (green circles), the results of *Escarpia southwardae* are provided for comparison (white squares; Bayon et al., 2020).

Compared with *E. southwardae*, the *P. echinospica* tube shows obvious negative Ce anomalies, positive yttrium (Y) anomalies, and enrichment of heavy REEs and seems to be more strongly affected by seawater (cf. Bayon et al., 2020). The occurrence of negative Ce anomalies between tube sections P1-P16 (except for P4 that shows slightly positive Ce anomaly) suggests that the anterior section of the tube has remained under oxic bottom-water conditions during the lifetime of the tubeworm. On the contrary, positive Ce anomalies appear in the tube's

posterior end (P17 and P19) where the tubeworm plunges into the sediment and hydrogen sulfide is presumably taken up from anoxic pore waters for the nutrition needs of the endosymbiotic thiotrophs. The negative Ce anomalies of P18 in the posterior part of the tube possibly indicates that the tube itself acts as a direct conduit for seawater sulfate down to the reduced subsurface environment – a mechanism that has been previously inferred to play an important role in sustaining high production rates of dissolved sulfide, enabling the development of dense bushes of tubeworms over long periods of time (Cordes et al., 2005).

## REFERENCES CITED

- Alibo, D.S., and Nozaki, Y., 2000, Dissolved rare earth elements in the South China Sea: Geochemical characterization of the water masses. *Journal of Geophysical Research*, v. 105, p. 28771–28783, <https://doi.org/10.1029/1999JC000283>.
- Anbar, A.D., 2004, Molybdenum stable isotopes: observations, interpretations, directions. *Reviews in Mineralogy and Geochemistry*, v. 55, p. 429–454, <https://doi.org/10.2138/gsrmg.55.1.429>.
- Chen, S., Peng, X.-T., Li, J., Lin, Z., Li, H.-Y., Wei, G.-J., Li, X., Ta, K.-W., Dasgupta, S., Xu, H.-C., Du, M.-R., Li, J.-W., Liu, Y., Zhou, J.-L., Liu, S.-Q., and Zhang, J., 2022, Extremely light molybdenum isotope signature of sediments in the Mariana Trench. *Chemical Geology*, v. 605, 120959, <https://doi.org/10.1016/j.chemgeo.2022.120959>.
- Cordes, E.E., Arthur, M.A., Shea, K., Arvidson, R.S., and Fisher, C.R., 2005, Modeling the mutualistic interactions between tubeworms and microbial consortia. *PLoS*

Biology, v. 3, e77, <https://doi.org/10.1371/journal.pbio.0030077>.

Guan, H., Birgel, D., Feng, D., Peckmann, J., Liu, L., Liu, L., and Tao, J., 2021, Lipids and their  $\delta^{13}\text{C}$  values reveal carbon assimilation and cycling in the methane-seep tubeworm *Paraescarpia echinospica* from the South China Sea. Deep-Sea Research I, v. 174, 103556, <https://doi.org/10.1016/j.dsr.2021.103556>.

Kendall, B., Dahl, T.W., and Anbar, A.D., 2017, The stable isotope geochemistry of molybdenum. Reviews in Mineralogy and Geochemistry, v. 82, p. 683–732, <https://doi.org/10.2138/rmg.2017.82.16>.

Li, J., Liang, X.-R., Zhong, L.-F., Wang, X.-C., Ren, Z.-Y., Sun, S.-L., Zhang, Z.-F., and Xu, J.-F., 2014, Measurement of the isotopic composition of molybdenum in geological samples by MC-ICP-MS using a novel chromatographic extraction technique. Geostandards and Geoanalytical Research, v. 38, p. 345–354, <http://dx.doi.org/10.1111/j.1751-908X.2013.00279.x>.

Luo, J., Long, X., Bowyer, F.T., Mills, B.J.W., Li, J., Xiong, Y., Zhu, X., Zhang, K., and Poulton, S.W., 2021, Pulsed oxygenation events drove progressive oxygenation of the early Mesoproterozoic ocean. Earth and Planetary Science Letters, v. 559, 116754, <https://doi.org/10.1016/j.epsl.2021.116754>.

Pourmand, A., Dauphas, N., and Ireland, T.J., 2012, A novel extraction chromatography and MC-ICP-MS technique for rapid analysis of REE, Sc and Y: Revising CI-chondrite and Post-Archean Australian Shale (PAAS) abundances. Chemical Geology, v. 291, p. 38–54, <https://doi.org/10.1016/j.chemgeo.2011.08.011>.

Siebert, C., Nägler, T.F., von Blanckenburg, F., and Kramers, J.D., 2003, Molybdenum isotope records as a potential new proxy for paleoceanography. *Earth and Planetary Science Letters*, v. 211, p. 159–171, [https://doi.org/10.1016/S0012-821X\(03\)00189-4](https://doi.org/10.1016/S0012-821X(03)00189-4).

Southward, E.C., Schulze, A., and Tunnicliffe, V., 2002, Vestimentiferans (Pogonophora) in the Pacific and Indian Oceans: a new genus from Lihir Island (Papua New Guinea) and the Java Trench, with the first report of *Arcovestia ivanovi* from the North Fiji Basin. *Journal of Natural History*, v. 36, p. 1179–1197, <https://doi.org/10.1080/00222930110040402>.

Sun, Y., Sun, J., Yang, Y., Lan, Y., Ip, J.C.-H., Wong, W.C., Kwan, Y.H., Zhang, Y., Han, Z., Qiu, J.-W., and Qian, P.-Y., 2021, Genomic signatures supporting the symbiosis and formation of chitinous tube in the deep-sea tubeworm *Paraescarpia echinospica*. *Molecular Biology and Evolution*, v. 38, p. 4116–4134, <http://dx.doi.org/10.1093/molbev/msab203>.

Thoby, M., Konhauser, K.O., Fralick, P.W., Altermann, W., Visscher, P.T., and Lalonde, S.V., 2019, Global importance of oxic molybdenum sinks prior to 2.6 Ga revealed by the Mo isotope composition of Precambrian carbonates. *Geology*, v. 47, p. 559–562, <https://doi.org/10.1130/G45706.1>.

Voegelin, A.R., Nägler, T.F., Samankassou, E., and Villa, I.M., 2009, Molybdenum isotopic composition of modern and Carboniferous carbonates. *Chemical Geology*, v. 265, p. 488–498, <https://doi.org/10.1016/j.chemgeo.2009.05.015>.

Wang, Z., Li, J., Wei, G., Deng, W., Chen, X., Zeng, T., Wang, X., Ma, J., Zhang, L.,

Tu, X., Wang, Q., and McCulloch, M., 2019, Biologically controlled Mo isotope fractionation in coral reef systems. *Geochimica et Cosmochimica Acta*, v. 262, p. 128–142, <https://doi.org/10.1016/j.gca.2019.07.037>.

Zerkle, A.L., Scheiderich, K., Maresca, J.A., Liermann, L.J., and Brantley, S.L., 2011, Molybdenum isotope fractionation by cyanobacterial assimilation during nitrate utilization and N<sub>2</sub> fixation. *Geobiology*, v. 9, p. 94–106, <https://doi.org/10.1111/j.1472-4669.2010.00262.x>.

Zhang, L., Ren, Z.-X., Xia, X.-P., Li, J., and Zhang, Z.-F., 2015, IsotopeMaker: A Matlab program for isotopic data reduction. *International Journal of Mass Spectrometry*, v. 392, p. 118–124, <http://dx.doi.org/10.1016/j.ijms.2015.09.019>.